ELSEVIER

Journal of Molecular Catalysis A: Chemical 185 (2002) 71–80

JOURNAL OF MOLECULAR CATALYSIS A: CHEMICAL

www.elsevier.com/locate/molcata

Benzylic oxidation with H_2O_2 catalyzed by Mn complexes of *N*,*N*′,*N*″-trimethyl-1,4,7-triazacyclononane: spectroscopic investigations of the active Mn species

T.H. Bennur, S. Sabne, S.S. Deshpande, D. Srinivas*, S. Sivasanker

Catalysis Division, National Chemical Laboratory, Pune 411008, India

Received 6 November 2001; accepted 25 March 2002

Abstract

Mn complexes of *N*,*N*′,*N*″-trimethyl-1,4,7-triazacyclononane (Mn–tmtacn) exhibit good catalytic activity, at ambient temperatures, for the benzylic oxidation of aromatics selectively to the corresponding alcohol and carbonyl compounds with H_2O_2 as oxidant in the presence of carboxylate buffers. The active Mn species in the reaction medium was investigated by UV–visible (UV–Vis), FT-IR–attenuated total reflectance (FT-IR–ATR) and electron spin resonance (ESR) spectroscopic techniques. The studies revealed the formation of terminal oxo- and μ-oxo-Mn(IV)–tmtacn complexes during the reaction. The oxo-manganese complexes and the nature of the carboxylic acid play an important role in the activation of the benzylic C–H bond.

Keywords: Manganese complexes; Mn–tmtacn; Selective oxidation; Benzylic oxidation; Oxidation with H_2O_2; ESR; Spectroscopic investigations

1. Introduction

The manganese complexes of *N*,*N*′,*N*″-trimethyl-1,4,7-triazacyclononane (Mn–tmtacn) have been reported to exhibit remarkable catalytic activity in the presence of carboxylate buffers in the stereo-selective epoxidation of olefins, epoxidation of terminal and electron deficient olefins and oxidation of alkanes and alcohols, with H_2O_2, at ambient temperatures [1–5]. The activity of Mn–tmtacn has been reported to depend on the nature of the carboxylate buffer. De Vos et al. [6,7] found high selectivity and conversion for the epoxidation reaction in the presence of an oxalate buffer. Shul'pin et al. [8,9] have reported high turnover numbers for alkane oxidation in the presence of acetic acid. The reason for the differences in activity observed in different carboxylate buffers perhaps arises from differences in the structures of the active Mn species involved in the oxidation reaction.

The activity of the Mn–tmtacn system in benzylic oxidation of aromatics is not yet reported. Many benzylic oxidation products are commercially important as fragrance materials and in the preparation of optically active α-amino acids [10]. Our observations reveal that Mn–tmtacn–H_2O_2 is unique for benzylic C–H bond oxidation of aromatics compared to the earlier reported catalysts [11–16], in that, it is efficient even at ambient temperatures. Commercial processes for C–H bond activation use cobalt-bromide ion catalyst in acetic acid medium and are carried out at a high temperature (∼500 K) and oxygen pressure (∼30 bar) [11]. The C–H bond oxidation reactions when carried out with cerium ammonium nitrate in

* Corresponding author. Tel./fax: +91-20-589-3761.
E-mail address: srinivas@cata.ncl.res.in (D. Srinivas).

1381-1169/02/$ – see front matter
PII: S1381-1169(02)00132-2

hot acetic acid, HNO_3 and $HClO_4$, Ce(IV)-triflate with water and oxo-Ru-porphyrin catalysts give only low yields [12–15] of the intermediate oxidation products. Choudary et al. [17] have obtained high yields of benzylic products by using Cr-PILC catalysts and *tert*-butyl hydroperoxide.

We report here the benzylic oxidation of ethylbenzene (EB), diethylbenzene (DEB), *o*-xylene (OX), and *m*-phenoxytoluene (MPT), at low temperatures (273–333 K) using Mn–tmtacn catalyst and H_2O_2 oxidant. The activity and selectivity of the catalyst in the presence of various buffers such as acetate, oxalate, tartrate, malonate, citrate and ascorbate are investigated. The structure of the active Mn species in different buffers is identified by in situ UV–Visible (UV–Vis), FT-IR–attenuated total reflectance (FT-IR–ATR) and electron spin resonance (ESR) spectroscopic studies.

2. Experimental

2.1. Materials and catalyst preparation

The ligand tmtacn was procured from Sigma–Aldrich, USA. $MnSO_4$, carboxylic acids (acetic acid, malonic acid, oxalic acid, tartaric acid, and citric acid), ascorbic acid and CH_3CN (A.R.) were obtained from s.d. fine chem. Ltd., India. The sodium salts of the above acids were prepared by reacting the corresponding acids with stoichiometric amounts of NaOH.

The catalyst system was prepared in situ in the catalytic reaction [6,7] by mixing $MnSO_4$, tmtacn and carboxylate buffer (prepared by mixing equimolar amounts of carboxylic acid and its sodium salt) in the ratio of 2:3:3 μmol in CH_3CN and distilled water mixture. The pH of the buffers were: acetate, 4.5; tartrate, 5.3; malonate, 6.0; oxalate, 5.4; ascorbate, 5.9 and citrate, 5.0.

2.2. Spectroscopic measurements

The ESR spectra were recorded on a Bruker EMX spectrometer operating at X-band frequency ($\nu \approx 9.74$ GHz) and 100 kHz field modulation. Measurements in solutions, at 298 K, were performed using a quartz aqueous cell. Microwave frequency was calibrated using a frequency counter built in the microwave-bridge (Bruker ER 041 XG-D). The magnetic field was calibrated with a Gaussmeter (Bruker ER 035 M NMR). Spectral simulations were carried out using the Bruker Simfonia software package. Spectral manipulations were done using the WINEPR software package. The UV–Vis spectra of the reaction mixture were recorded on a Shimadzu UV-2550 spectrophotometer in the region 200–900 nm. The FT-IR spectra of solutions were recorded on a Shimadzu 8201 PC spectrophotometer in the region 400–4000 cm^{-1} using a ZnSe ATR circle cell.

2.3. Reaction procedure and product analysis

The catalyst system was prepared in situ and used in the benzylic oxidation reactions. $MnSO_4 \cdot H_2O$ (2 μmol) dissolved in 0.1 ml of water was taken in a 25 ml double-necked round bottom flask fitted with a water cooled condenser. To this, 3 μmol of tmtacn in 0.1 ml of CH_3CN and 3 μmol of the carboxylate or ascorbate buffer were added. Then, 0.5 mmol of substrate was added followed by 0.8 ml of CH_3CN. The reactor was placed in a suitable bath and the reaction was conducted at 273–333 K by adding 0.3 ml of aqueous H_2O_2 (38%) diluted with 0.2 ml of CH_3CN over a 20 min period. The reaction was monitored by GC (Varian 3400; CP-SIL8CB column; 30 m × 0.53 mm) and the products were identified by GC–MS (Shimadzu QP 5000; DB1 column, 30 m × 0.25 mm) and GC–IR (Perkin Elmer 2000; BP-1 column, 25 m × 0.32 mm).

3. Results and discussion

3.1. Oxidation of EB

Mn–tmtacn–H_2O_2 system is efficient and selective for benzylic C–H bond oxidation of EB (Table 1). No β-C–H bond oxidation was noticed. 1-Phenylethanol (PhEtOH) and acetophenone (AcPh) were the major oxidation products. *Ortho*- and *para*-ring hydroxylated products were also observed. The reaction did not proceed in the absence of Mn–tmtacn complex. $VOSO_4$ and $FeSO_4$ failed to replace $MnSO_4$ in the catalyst system. The Mn system with no methyl substitution in the cyclic triaza ligand (Mn-tacn) was much less active (13 wt.% EB conversion in 8 h at

Table 1
Catalytic activity of Mn–tmtacn–H_2O_2 in the oxidation of EB[a]

Buffer	Reaction time (h)	Conversion (wt.%)	TOF[b]	Benzylic selectivity[c] (wt.%)	Selectivity (wt.%)[d]	
					PhEtOH	AcPh
Acetate	0.5	8.7	44	76.7	25.7	51.0
	10	18.8	4.7	68.4	21.5	46.9
Tartrate	0.5	14.7	74	84.4	23.5	60.9
	10	27.9	7.0	79.9	20.7	59.2
Malonate	0.5	26.2	130	85.0	0.0	85.0
	10	54.4	13.6	83.2	0.0	83.2
Oxalate	0.5	27.0	136	57.3	12.3	45.0
	10	69.0	17.3	60.2	19.4	40.8
Ascorbate	0.5	27.6	138	91.0	0.0	91.0
	10	59.1	14.8	83.5	0.0	83.5
Citrate	0.5	37.4	188	83.9	0.0	83.9
	10	52.3	13.0	85.2	17.9	67.3
No buffer	0.5	1.5	8	32.6	0.0	32.6
	10	6.5	1.6	70.3	0.0	70.3

[a] Reaction conditions: EB = 0.5 mmol; aq. H_2O_2 (38%) = 5 mmol; CH_3CN = 1 ml; H_2O = 0.1 ml; $MnSO_4$ = 2 μM; tmtacn = 3 μM; buffer = carboxylic acid (3 μM) + corresponding Na salt (3 μM); temperature = 313 K.
[b] Number of moles of EB converted per mole of catalyst per hour.
[c] Combined selectivity of PhEtOH and AcPh. Rest are ring hydroxylated products.
[d] PhEtOH, 1-phenylethanol; AcPh, acetophenone.

313 K with 43.5 wt.% benzylic selectivity in oxalate buffer) compared to Mn–tmtacn (Table 1).

3.1.1. Effect of temperature

Fig. 1 shows the effect of temperature on EB oxidation activity of Mn–tmtacn–H_2O_2 system in the presence of the oxalate buffer. The conversion of EB was low at 273 K (3.8 wt.%) and 301 K (14.5 wt.%), but the benzylic product selectivity was high at these temperatures (88.4 wt.%). The conversion increased with temperature up to 313 K and then decreased with a further increase in the temperature (Fig. 1). At 333 K, both the conversion (27 wt.%) and product selectivity (55 wt.%) were low due to decomposition of H_2O_2 and formation of ring hydroxylated products, respectively. Higher activity and selectivity were observed at 313 K. Thus, all the reactions discussed in the following sections were carried out at 313 K only.

3.1.2. Effect of carboxylate buffer

The catalytic activity of Mn–tmtacn–H_2O_2 system for EB oxidation was studied in the presence of the carboxylate buffers acetate, malonate, oxalate, tartrate and citrate and a non-carboxylate ascorbate buffer. The results are listed in Table 1. Fig. 2a and b show, respectively, the conversion of EB and benzylic product selectivity obtained in different buffers as a function of run duration. It is noticed that the conversion was rapid during the first 0.5 h, nearly 40–70% of the total conversion (in 10 h) taking place during this period. The conversion was small in the absence of any buffer (Table 1). The activity of the catalyst system (EB conversion and turnover frequency (TOF)) at 0.5 h in different buffers varied in the following order: acetate < tartrate < malonate < oxalate ≤ ascorbate < citrate. The increase in EB conversion after 0.5 h was smaller in acetate, tartrate and citrate buffers than in oxalate and malonate buffers. At the end of 6 h, a higher conversion was observed in the oxalate buffer than in the other buffers. The system with oxalate buffer showed lower benzylic product selectivity (57 wt.%) compared to the other buffers (76–91 wt.%, 0.5 h; Table 1; Fig. 2b). The benzylic product selectivity decreased marginally after 1–4 h (depending on the

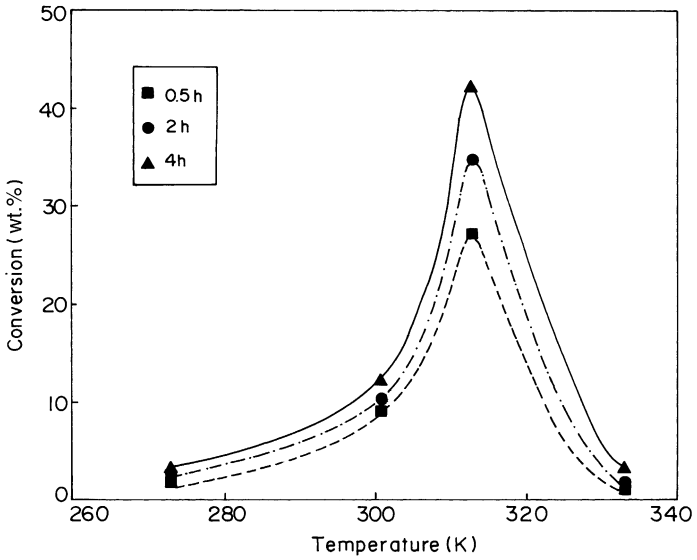

Fig. 1. Catalytic activity of Mn–tmtacn–oxalate–H_2O_2 system as a function of temperature.

buffer) due to an increase in the rate of other reactions and decomposition of buffer/complex (Fig. 2b). The malonate and ascorbate buffers were unique to yield only AcPh as the selective benzylic product while the rest of the buffers yielded both PhEtOH and AcPh (Table 1). This suggests that with the malonate and ascorbate buffers, the intermediate alcohol is rapidly oxidized to the ketone or a different type of oxidation mechanism is involved. In the absence of any buffer, the conversion of EB was small (6.5% at 10 h) and the ketone was the only product (Fig. 2 and Table 1).

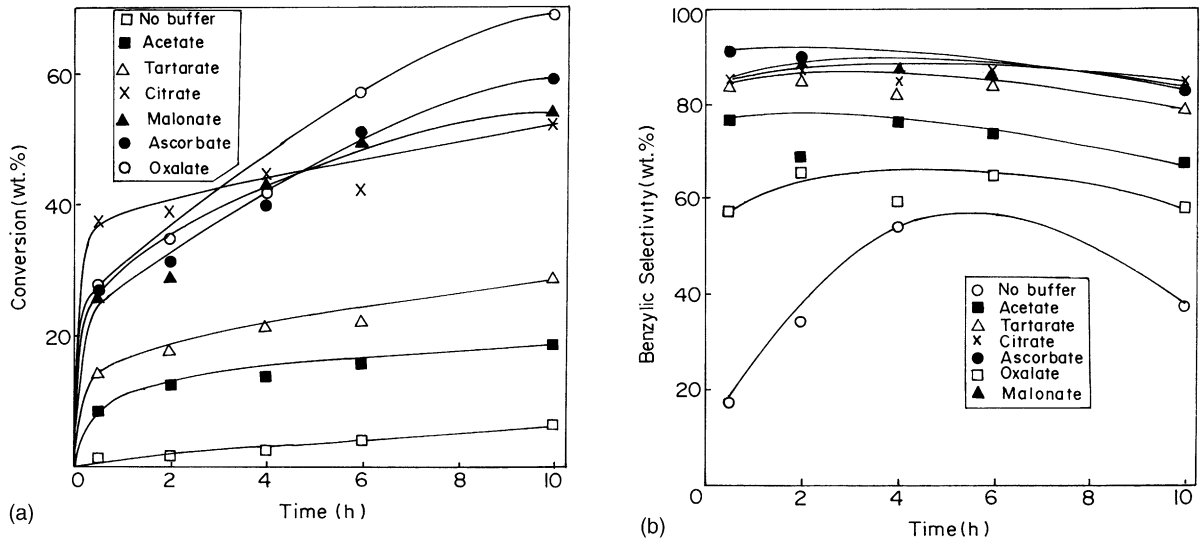

Fig. 2. Influence of carboxylic acid buffer on the activity of Mn–tmtacn–H_2O_2 system in the oxidation of EB.

Table 2
Benzylic oxidation of aromatic compounds by Mn–tmtacn–H_2O_2 system in oxalate and citrate buffers

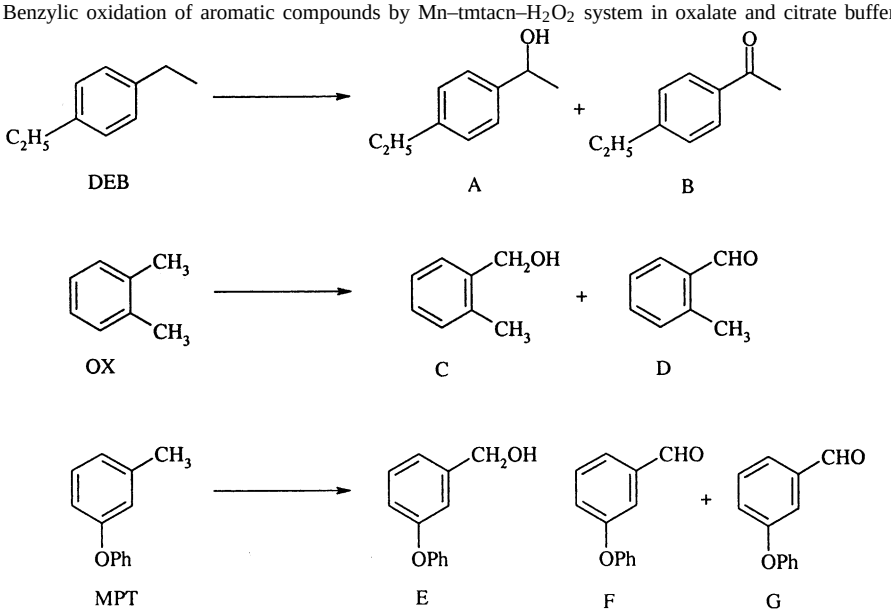

Substrate	Buffer	Time (h)	Conversion (wt.%)	TOF	Benzylic selectivity (wt.%)	Benzylic product distribution (wt.%)
DEB	Oxalate	0.5	25.1	125.4	67.8	A, 31.4; B, 36.4
		10	49.6	12.4	55.9	A, 25.3; B, 30.6
	Citrate	0.5	32.1	160.6	81.0	A, 33.1; B, 47.8
		10	35.1	8.8	78.5	A, 29.5; B, 49.0
OX	Oxalate	0.5	20.1	100.8	39.4	C, 13.9; D, 25.5
		10	77.4	19.3	44.9	C, 19.3; D, 25.6
	Citrate	0.5	14.5	71.8	55.0	C, 17.6; D, 37.4
		10	53.3	13.3	50.2	C, 10.2; D, 40.0
MPT	Oxalate	0.5	8.7	43.4	81.8	E, 30.9; F, 41.3; G, 9.7
		6	15.3	6.3	50.8	E, 19.0; F, 31.8; G, 6.0
	Citrate	0.5	7.4	37.0	72.1	E, 23.2; F, 42.7; G, 6.2
		10	12.2	3.0	80.5	E, 28.9; F, 41.5; G, 10.1

3.2. Oxidation of aromatic compounds

The catalytic activity data for the oxidation of DEB, OX and MPT in oxalate and citrate buffers are presented in Table 2. A maximum conversion of 77.4 wt.% was observed for OX, 49.6 wt.% for DEB and 15.3 wt.% for MPT in the oxalate buffer. Only one of the alkyl groups in DEB and OX could be oxidized. The ring hydroxylated products were more in OX oxidation. Substrate conversion was, in general, more in oxalate than in the citrate buffer, though the benzylic product selectivity was lower than in the latter buffer.

3.3. In situ spectroscopic studies

3.3.1. UV–Vis spectroscopy

UV–Vis spectra of Mn–tmtacn–H_2O_2 were recorded in the presence of acetate and oxalate buffers (Fig. 3(i) and (ii)). The Mn–tmtacn complex in CH_3CN–H_2O mixture showed broad, partially resolved UV bands of ligand origin at around 310 and

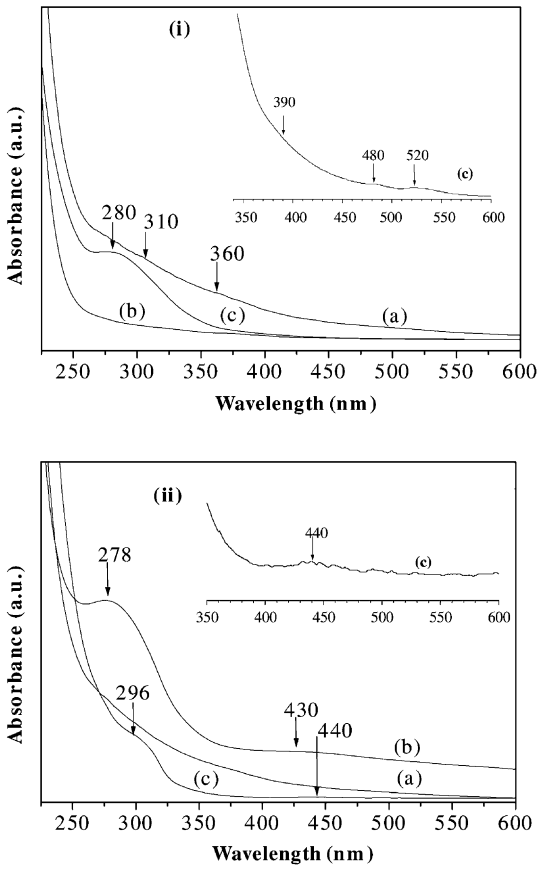

Fig. 3. UV–Vis spectra in CH_3CN–H_2O: (i)—(a) $MnSO_4$ + tmtacn, (b) $MnSO_4$ + tmtacn + acetate buffer, (c) $MnSO_4$ + tmtacn + acetate buffer + H_2O_2; (ii)—(a) $MnSO_4$ + tmtacn, (b) $MnSO_4$ + tmtacn + oxalate buffer and (c) $MnSO_4$ + tmtacn + oxalate buffer + H_2O_2. Inset shows the blow-up of traces (c).

360 nm (Fig. 3(i), curve a). The intensity of these bands decreased in the presence of acetate buffer (Fig. 3(i), compare curve b with curve a). Upon adding H_2O_2 to Mn–tmtacn–acetate system, a new, intense band was observed at 280 nm (Fig. 3(i), curve c), in addition to three weak bands at 390, 480 and 520 nm (Fig. 3(i), inset). The former (at 280 nm) is attributed to carboxylate to Mn charge transfer band and those bands at 480 and 520 nm are due to d–d transitions.

Soon after adding the oxalate buffer a marked change was noted in the spectrum of Mn–tmtacn (Fig. 3(ii), compare curves b and a); a strong band at 278 nm and a weak, broad band at 430 nm were observed. Such bands were not seen in acetate buffer indicating the formation of a different kind of Mn–tmtacn complex in oxalate compared to that in acetate buffer. This is further substantiated by ESR spectroscopy (vide infra). However, on adding H_2O_2 these bands disappeared and two new bands appeared at 296 and 440 nm (Fig. 3(ii), curve c and inset). A comparative study with similar Mn complexes [18,19] reveals that the weak band at 440 nm in Mn–tmtacn–oxalate–H_2O_2 is due to the formation of a terminal oxo-manganese complex, (tmtacn)(oxalate)Mn=O and the band at 390 nm in Mn–tmtacn–acetate–H_2O_2 is due to μ-oxo manganese complex, (μ-O)(μ-acetato)$_2$Mn$_2$(tmtacn)$_2$. The different oxo-manganese species account for the difference in activity of the Mn–tmtacn system in different buffers. The formation of oxo-manganese complexes was confirmed also from FT-IR–ATR and ESR investigations.

3.3.2. FT-IR spectroscopy

The FT-IR–ATR spectrum of Mn–tmtacn–oxalate–H_2O_2 in CH_3CN–H_2O is shown in Fig. 4. The coordinated oxalate exhibits characteristic IR bands at 1612 and 1361 cm^{-1} due to carboxylato stretching modes. The bands at 1146 and 1201 cm^{-1} are due to SO_4^{2-} ions. Upon adding H_2O_2 to Mn–tmtacn–oxalate, weak partially resolved bands were observed at around 1090, 975 and 806 cm^{-1}. Similar optical features (at 412 nm in UV–Vis and 979 cm^{-1} in FT-IR) were reported earlier for terminal oxo-Mn-porphyrin complexes [18,19].

3.3.3. ESR spectroscopy

$MnSO_4$ dissolved in CH_3CN–H_2O mixture showed characteristic, well resolved Mn hyperfine features centered at g_{iso} = 2.002 (A_{iso}(Mn) = 95.6 G; line width (ΔH_{pp}) = 32 G; Fig. 5a). The intensity of Mn signals decreased on adding tmtacn ligand (Fig. 5b). However, on adding acetate buffer to the Mn–tmtacn solution the original spectral intensity (Fig. 5c) was regained (ΔH_{pp} = 55 G). Addition of substrate (EB) had little effect on the spectrum (Fig. 5d), but, when H_2O_2 was added, the line width of the Mn signals reduced to 40 G (Fig. 5e). The ESR results are interpreted as follows. When $MnSO_4$ and tmtacn were mixed Mn(II)–tmtacn complex was formed. This was highly reactive towards aerial oxygen. A

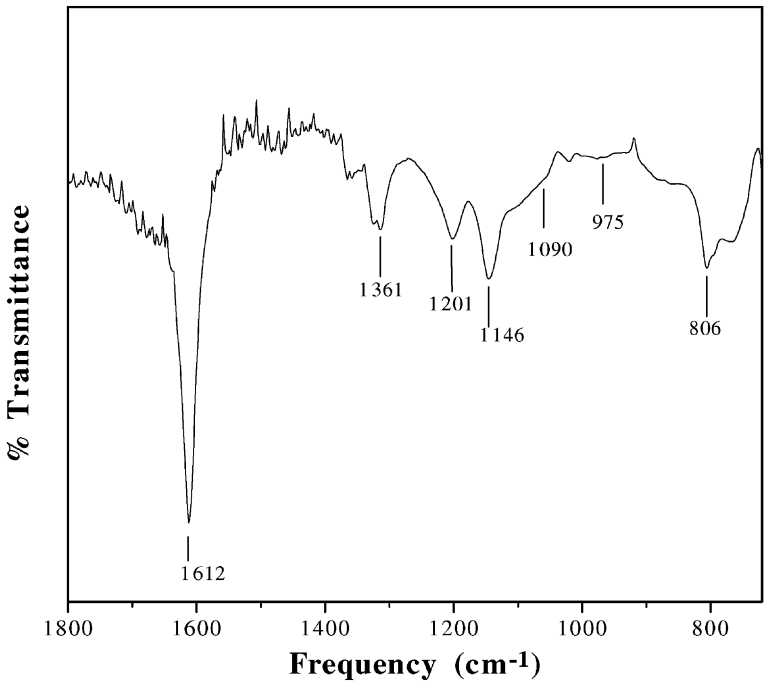

Fig. 4. FT-IR–ATR spectrum of $MnSO_4$–tmtacn–oxalate buffer–H_2O_2 in CH_3CN–H_2O solution.

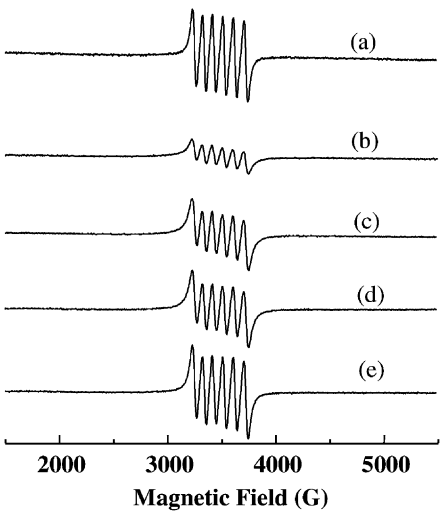

Fig. 5. ESR spectra in CH_3CN–H_2O at 298 K: (a) $MnSO_4$, (b) $MnSO_4$ + tmtacn, (c) $MnSO_4$ + tmtacn + acetate buffer, (d) $MnSO_4$ + tmtacn + acetate buffer + EB and (e) $MnSO_4$ + tmtacn + acetate buffer + EB + H_2O_2.

part of it was converted into an ESR-silent Mn(III) species and as a consequence of this, the overall spectral intensity of $MnSO_4$–tmtacn decreased. The line width of Mn(II)–tmtacn (60 G) was more than that of $MnSO_4$ solution (32 G) (Fig. 5b) suggesting weak intermolecular interactions in the former solution. In acetate buffer, Mn was in +2 oxidation state as Mn(II)–tmtacn–acetate complex. However, on adding H_2O_2, a binuclear μ-oxo-manganese(IV) (designated as species A) was formed. Such μ-oxo-Mn complexes were isolated and structurally characterized by Wieghardt and co-workers [20–22] and Koek et al. [23].

Marked changes were observed in the spectra of Mn–tmtacn complex in oxalate buffer. Mn–tmtacn in oxalate buffer exhibited an intense signal at $g_{iso} = 2.0012$ with $\Delta H_{pp} = 33.6$ G (Fig. 6a); no Mn hyperfine features were observed. The origin of this signal was due to a radical attached to Mn(III) center. The intensity of the radical signal decreased on adding EB (Fig. 6b) and weak Mn(II) hyperfine could be seen due to interaction of the radical species with EB. On adding H_2O_2 the radical species disappeared and a signal with

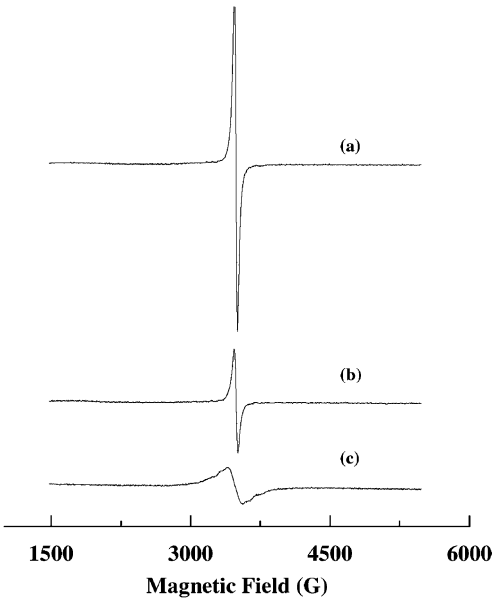

Fig. 6. ESR spectra in CH_3CN–H_2O at 298 K. (a) $MnSO_4$ + tmtacn + oxalate buffer, (b) $MnSO_4$ + tmtacn + oxalate buffer + EB and (c) $MnSO_4$ + tmtacn + oxalate buffer + EB + H_2O_2.

$\Delta H_{pp} = 190$ G (Fig. 6c) due to terminal oxo-Mn(IV) complex (designated as species B) appeared.

In other buffers, on adding H_2O_2, spectra corresponded to both species A and B (exhibiting overlapped Mn hyperfine features with the broad signal). The relative amounts of these species were different in different buffers. Fig. 7 shows the experimental and simulated spectra of the system in the presence of malonate buffer. The ESR signal intensity variations of species A and B in different buffers are shown in Fig. 8.

4. Structure–activity relations

The following conclusions are drawn from the spectroscopic studies. Carboxylic acid acts as co-ligand in addition to acting as a buffer. Carboxylato-bridged complexes have been identified as active sites in metalloenzymes [24]. The nature of the carboxylic acid group and mode of coordination influence the redox behavior of the Mn site. In the presence of acetate, malonate and tartrate, Mn–tmtacn forms carboxylato-bridged complexes of type (**I**) shown in Fig. 9 [20–22]. However, in oxalate buffer, Mn(II)

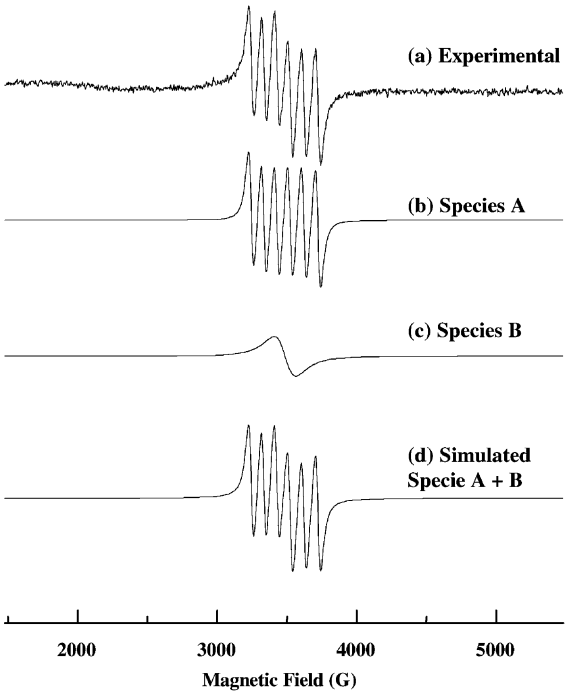

Fig. 7. Experimental and simulated ESR spectra of $MnSO_4$–tmtacn–malonate–EB–H_2O_2 system in CH_3CN–H_2O mixture at 298 K.

is oxidized to Mn(III) with a concomitant reduction of oxalate yielding (tmtacn)Mn^{III}(oxalate$^{\bullet -}$) radical complex (**II**; Fig. 9). Such radical intermediates were identified also in the oxidation reactions involving metal porphyrins [25]. Addition of H_2O_2 forms μ-oxo- (species A) and terminal-oxo- (Species B) Mn(IV) complexes (Fig. 8). The former type of complexes are characterized by resolved Mn hyperfine pattern (Fig. 5e) while the latter by a broad ESR signal at $g \sim 2$ at 298 K (Fig. 6c). In acetate, malonate and citrate buffers both A and B were co-existent. In the oxalate buffer species B was most predominant (Fig. 6) while species A was dominant in solutions containing acetate and tartrate buffers. The distinctive behavior of oxalate buffer is attributed to (i) its capability to influence the redox behavior of manganese, (ii) intramolecular electron transfer resulting in the formation of the carboxylato radical intermediates and (iii) formation of terminal oxo-Mn(IV) species. It is interesting to note that Mn–tmtacn exhibits good activity even in the presence of the non-carboxylic acid ascorbate buffer. This suggests that ascorbate too

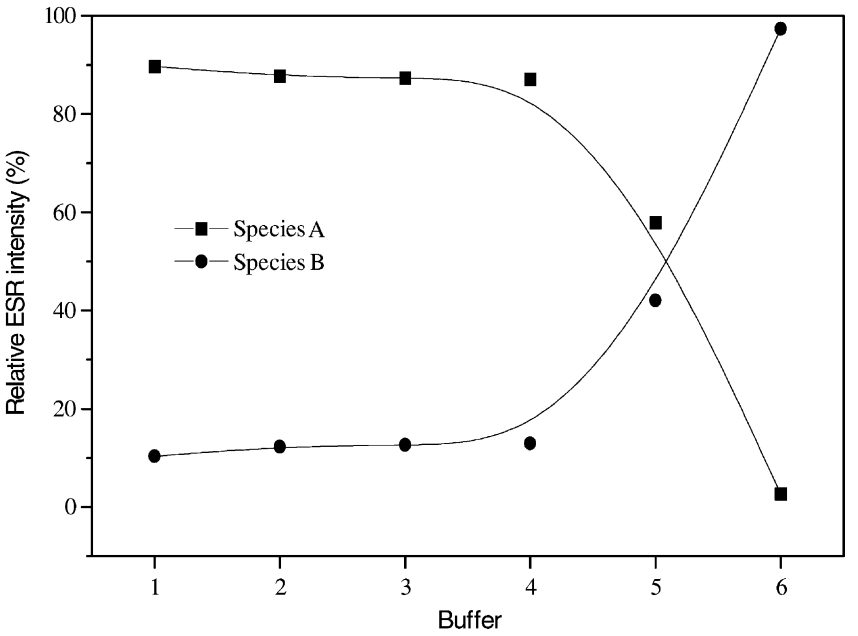

Fig. 8. ESR signal intensity (%) of species A and B in Mn–tmtacn–H_2O_2 in the presence of carboxylic acid buffers: (1) acetate, (2) citrate, (3) ascorbate, (4) tartrate, (5) malonate and (6) oxalate.

can influence the redox behavior of Mn and form the active Mn species required for the benzylic oxidation.

Based on ESR and UV–Vis studies two types of oxo-manganese complexes, (μ-oxo)(μ-carboxylato)-$[Mn^{IV}$–tmtacn$]_2$ (species A) and terminal oxo-Mn^{IV}–tmtacn (species B) can be identified in the solutions after reactions with H_2O_2. Tentative structures of these oxo-manganese complexes are shown in Fig. 9. Although the teminal oxo-manganese complexes (species B) appeared to be the active species for benzylic oxidation, no linear correlation in catalytic activity with the concentration of A or B was noted.

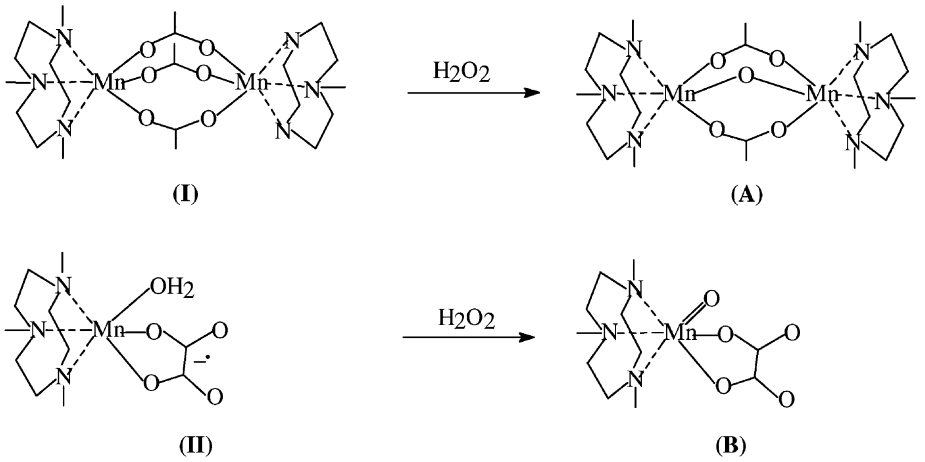

Fig. 9. Active Mn–tmtacn species in the presence of acetate and oxalate buffers.

This suggests that other factors such as the structure of the buffer and its mode of coordination also play an important role in the activity of oxo-manganese species.

5. Conclusions

The Mn–tmtacn complex exhibits superior activity for benzylic oxidation in the presence of oxalate, ascorbate and citrate buffers than in the presence of acetate, malonate and tartrate buffers. In situ spectroscopic studies reveal that oxo-manganese complexes, formed during the reaction catalyze the benzylic oxidation of aromatics. The nature of the buffer and its mode of coordination has a definite role in the activity of oxo-manganese complexes.

Acknowledgements

Authors thank Dr. S.G. Hegde for help in FT-IR analysis. THB thanks Council of Scientific and Industrial Research, New Delhi, for the award of Senior Research Fellowship.

References

[1] R. Hage, J.E. Iburg, J. Kerschner, J.H. Koek, E.L.M. Lempers, R.J. Martens, U.S. Racherla, S.W. Russell, T. Swarthoff, M.R.P. van Vliet, J.B. Warnaar, L. van der Wolf, B. Krijnen, Nature 369 (1994) 637.
[2] D.E. De Vos, T. Bein, Chem. Commun. (1996) 917.
[3] D.E. De Vos, T. Bein, J. Organomet. Chem. 195 (1996) 520.
[4] C. Zondervan, R. Hage, B.L. Feringa, Chem. Commun. (1997) 419.
[5] A. Berkessel, C.A. Sklorz, Tetrahedron Lett. 40 (1999) 7965.
[6] D.E. De Vos, B.F. Sels, M. Reynaers, Y.V. Subba Rao, P.A. Jacobs, Tetrahedron Lett. 39 (1998) 3221.
[7] D.E. De Vos, S. de Wildeman, B.F. Sels, P.J. Grobet, P.A. Jacobs, Angew. Chem. Int. Ed. 38 (1999) 980.
[8] J.R.L. Smith, G.B. Shul'pin, Tetrahedron Lett. 39 (1998) 4909.
[9] G.B. Shul'pin, G. Süss-Fink, L.S. Shul'pina, J. Mol. Catal. A 170 (2001) 17.
[10] M. O'Donnell, J.M. Boniece, S.E. Earp, Tetrahedron Lett. (1978) 2641.
[11] R.A. Sheldon, R.A. van Santen (Eds.), Catalytic Oxidation—Principles and Applications, World Scientific, Singapore, 1995.
[12] G.A. Molander, Chem. Rev. 92 (1992) 29.
[13] T.L. Ho, Synthesis (1973) 347.
[14] V. Nair, J. Mathew, J. Prabhakaran, Chem. Soc. Rev. 26 (1997) 127.
[15] K.K. Laali, M. Herbert, B. Cushnyr, A. Bhatt, D. Terrano, J. Chem. Soc., Perkin Trans. I (2001) 578.
[16] R. Zhang, W.-Y. Wu, T.-S. Lai, C.-M. Che, Chem. Commun. (1999) 1791.
[17] B.M. Choudary, A. Durgaprasad, V. Bhuma, V. Swapna, J. Org. Chem. 57 (1992) 5841.
[18] J.T. Groves, Y. Watanabe, Inorg. Chem. 25 (1986) 4808.
[19] T.J. Collins, R.D. Powell, C. Slebodwick, E.S. Uffelman, J. Am. Chem. Soc. 112 (1990) 897.
[20] K. Wieghardt, K.U. Bossek, B. Nuber, J. Weiss, J. Bouvoisin, M. Corbella, S.E. Vitols, J.-J. Girerd, J. Am. Chem. Soc. 110 (1988) 7398.
[21] K. Bossek, K. Wieghardt, B. Number, J. Weiss, Inorg. Chim. Acta 165 (1989) 123.
[22] J.R. Hartman, R.L. Rardin, P. Chaudhuri, K. Pohl, K. Wieghardt, B. Nuber, G.C. Papaefthymion, R.B. Frankel, S.J. Lippard, J. Am. Chem. Soc. 109 (1987) 7387.
[23] J.H. Koek, S.W. Russell, L. van der Wolf, R. Hage, J.B. Warnaar, A.L. Spek, J. Kerschner, L. DelPizzo, J. Chem. Soc., Dalton Trans. (1996) 353.
[24] R.C. Mehrotra, R. Bohra, Metal Carboxylates, Academic Press, New York, 1983.
[25] B. Meunier (Ed.), Metal-oxo and Metal-peroxo Species in Catalytic Oxidations, Vol. 97, Structure and Bonding 2000, Springer, Berlin.